Water Research 209 (2022) 117858

Contents lists available at ScienceDirect

Water Research

journal homepage: www.elsevier.com/locate/watres

Application of UV absorbance and electron-donating capacity as surrogates for micropollutant abatement during full-scale ozonation of secondary-treated wastewater

Nicolas Walpen [a], Adriano Joss [a], Urs von Gunten [a,b,c,*]

[a] Swiss Federal Institute of Aquatic Science and Technology (Eawag), 8600 Dübendorf, Switzerland
[b] Institute of Biogeochemistry and Pollutant Dynamics, ETH Zurich, 8092 Zurich, Switzerland
[c] School of Architecture, Civil and Environmental Engineering (ENAC), École Polytechnique Fédérale de Lausanne (EPFL), 1015 Lausanne, Switzerland

ARTICLE INFO

Keywords:
Ozonation
Micropollutant abatement
Electron-donating capacity
UV absorbance
On-line monitoring

ABSTRACT

Ozonation of secondary-treated wastewater for the abatement of micropollutants requires a reliable control of ozone doses. Changes in the UV absorbance of dissolved organic matter (DOM) during ozonation allow to estimate micropollutant abatement on-line and were therefore identified as feed-back control parameter. In this study, the suitability of the electron-donating capacity (EDC) as an additional surrogate parameter which is independent of optical DOM properties was evaluated during full-scale ozonation. For this purpose, a recently developed EDC analyzer was enhanced to enable continuous on-line EDC and UV absorbance measurements. During a multi-week monitoring campaign at the wastewater treatment plant of Zurich, Switzerland, specific ozone doses were varied from 0.13 to 0.91 $mg_{O3}{\cdot}mg_{DOC}{}^{-1}$ and selected micropollutants with different ozone reactivities were analyzed by LC-MS in conjunction with bromate analysis by IC-MS. In agreement with previous laboratory studies, the relative residual UV absorbance and EDC both decreased exponentially as a function of the specific ozone dose and, in comparison to the residual UV absorbance, residual EDC values showed a more pronounced decrease at low specific ozone doses $\leq$0.34 $mg_{O3}{\cdot}mg_{DOC}{}^{-1}$. Logistic regression models allowed to estimate relative residual micropollutant concentrations in the ozonation effluent using either the residual UV absorbance or EDC as explanatory variable. Averaging those models along the explanatory variables allowed to estimate target values in relative residual UV absorbances and EDC for specific micropollutant abatement targets. In addition, both parameters allowed to identify conditions with elevated conversions of bromide to bromate. Taken together, these findings show that the integration of relative residual EDC values as a second control parameter can improve existing absorbance-based ozonation control systems to meet micropollutant abatement targets, particularly for treatment systems where low ozone doses are applied.

1. Introduction

Ozonation is increasingly applied for enhanced wastewater treatment to oxidize a wide range of organic micropollutants thereby mitigating their discharge to the aquatic environment (Eggen et al., 2014; Völker et al., 2019; von Gunten, 2018). For this purpose, ozone (O_3) is dosed to secondary-treated wastewater, where it selectively oxidizes micropollutants containing electron-rich moieties such as olefins, activated aromatics including phenols, and neutral amines (Bourgin et al., 2018; Hollender et al., 2009; Lee and von Gunten, 2010). At the same time, O_3 also reacts with dissolved organic matter (DOM) and dissolved inorganic compounds forming hydroxyl radical ($^{\bullet}OH$), a less selective oxidant, which also contributes to the oxidation of micropollutants and DOM (Buffle et al., 2006b; Buffle and von Gunten, 2006; Nöthe et al., 2009; Remucal et al., 2020). The extent of micropollutant abatement is primarily determined by the exposure of the oxidants O_3 and $^{\bullet}OH$ (i.e., O_3 and $^{\bullet}OH$ concentrations integrated over time) and the rate constants of the reactions of these micropollutants with O_3 and $^{\bullet}OH$ (Lee et al., 2013). Oxidant exposures not only depend on the O_3 doses but also on complex reaction systems involving DOM and inorganic compounds such as nitrite (Lee et al., 2013; Schindler Wildhaber et al., 2015; von Sonntag and von Gunten, 2012). At the same time, excessive oxidant exposures can cause the formation of problematic oxidation by-products such as bromate, a possible carcinogen and regulated drinking water

* Corresponding author.
E-mail address: vongunten@eawag.ch (U. von Gunten).

https://doi.org/10.1016/j.watres.2021.117858
Received 15 July 2021; Received in revised form 19 October 2021; Accepted 8 November 2021
Available online 12 November 2021

contaminant (Soltermann et al., 2016; von Gunten and Hoigné, 1994). In addition, the production of O_3 consumes significant amounts of electrical energy (Katsoyiannis et al., 2011). Overall, an accurate and reliable control of applied O_3 doses is critical to reach optimal oxidant exposures and an energy-efficient abatement of micropollutants with a minimal formation of oxidation by-products.

Because on-line predictions or measurements of oxidant exposures and micropollutant concentrations are unfeasible in secondary-treated wastewater, changes in optical DOM properties have been suggested as surrogate parameters for micropollutant abatement during full-scale ozonation (Bahr et al., 2007; Deniere et al., 2021; Dickenson et al., 2009; Gerrity et al., 2012; Stapf et al., 2016; Wittmer et al., 2015). Ozonation-induced decreases of the UV absorbance and fluorescence of DOM reflect the oxidation of chromophoric DOM moieties (von Sonntag and von Gunten, 2012; Wenk et al., 2013; Wert et al., 2009a; Westerhoff et al., 1999). Numerous studies have reported correlations between relative decreases in UV absorbances and the abatement of individual micropollutants (Bahr et al., 2007; Buffle et al., 2006a; Dickenson et al., 2009; Gerrity et al., 2012; Nanaboina and Korshin, 2010; Song et al., 2021; Wert et al., 2009b). These relative decreases in UV absorbance proved to be suitable surrogate parameters for the on-line estimation of micropollutant abatement and control of O_3 doses in secondary-treated municipal wastewater (Stapf et al., 2016; Wittmer et al., 2015). Besides changes in UV absorbance, effects of ozonation on fluorescence signals have also been explored and used to expand existing surrogate models for the estimation of micropollutant abatement (Chys et al., 2017; Gerrity et al., 2012). While these approaches proved useful, the availability of a second surrogate parameter which is independent of optical DOM properties would be beneficial to increase the accuracy, reliability and resilience of existing on-line process monitoring and control systems for the ozonation of secondary-treated wastewater.

In laboratory experiments, the electron-donating capacity (EDC) of DOM was shown to potentially serve as such an additional, independent surrogate parameter (Chon et al., 2015). The EDC is operationally defined as the number of electrons transferred from DOM to an oxidant at a constant pH and reduction potential E_H (Aeschbacher et al., 2010). With the radical cation of 2,2′-azino-bis(3-ethylbenzthiazoline-6-sulphonate) ($ABTS^{\bullet+}$) as oxidant, EDC values were demonstrated to be a measure for the content of phenolic moieties of DOM (Aeschbacher et al., 2012). $ABTS^{\bullet+}$ can be prepared through a chemical or electrochemical one-electron oxidation of ABTS and can be detected electrochemically or photometrically, e.g. at an absorption maximum at 730 nm (Aeschbacher et al., 2012; Chon et al., 2015; Scott et al., 1993; Walpen et al., 2016). Because ozonation of DOM leads to the oxidation of phenolic moieties (Ramseier and von Gunten, 2009; Remucal et al., 2020; Tentscher et al., 2018), EDC values decrease in parallel to the abatement of UV absorbances (Chon et al., 2015; Önnby et al., 2018; Wenk et al., 2013). During the ozonation of secondary-treated wastewater samples, decreases in EDC also correlated with the abatement of spiked micropollutants (Chon et al., 2015). However, these observations were only a proof of concept and limited to a small number of micropollutants and, because of the lack of automated devices for the quantification of EDC, limited to a few laboratory ozonation experiments. To advance the analytical techniques and to enable a continuous on-line monitoring of changes in EDC and UV absorbance, we have recently developed an EDC analyzer and validated the analyzer in the laboratory (Walpen et al., 2020). Yet, the EDC analyzer required further development for an entirely automated, on-site operation. For this, several practical issues have to be addressed including (i) the continuous supply with filtered sample solution, (ii) a more rugged fluidic system suitable for an industrial environment, and (iii) a robust and resilient device control. Because of the lack of an appropriate analytical device, a systematic study correlating continuously measured decreases in EDC and the abatement organic micropollutants during full-scale ozonation to evaluate EDC as a surrogate parameter under realistic conditions is still missing.

To address this gap, this study assesses the suitability of on-line EDC measurements in comparison to UV absorbance measurements as surrogate parameter for micropollutant abatement during the full-scale ozonation at a municipal wastewater treatment plant. For this purpose, the previously developed EDC analyzer was further improved and completely automated to enable on-line measurements of changes in EDC and UV absorbance. Compared to the previously presented analyzer (Walpen et al., 2020), the new device additionally included sample filtration modules, a more robust fluidic system mounted to a mobile platform wagon, and was completely automated using an industry-grade programmable logical controller for continuous sampling and measurement. A repeated analysis of a batch of influent and effluent of the ozonation reactors was performed to assess the analytical performance of the analyzer and it was applied to continuously monitor the residual UV absorbance and EDC during full-scale ozonation. During this monitoring campaign, O_3 doses were varied and the resulting abatement of 22 selected micropollutants and formation of bromate were quantified in grab samples. To assess on-line EDC measurements as surrogate parameter for micropollutant abatement, regression models using either the residual UV absorbance or EDC to estimate residual micropollutant concentrations were compared.

2. Material and methods

2.1. Chemicals and solutions for the EDC analyzer

The EDC analyzer was supplied with two reactant solutions containing ABTS and chlorine, respectively, a phosphate buffer solution as well as deionized water and a 2-propanol-water mixture (50% v/v). Aliquots of the ABTS and chlorine solutions were automatically mixed during every measurement cycle to yield the oxidative reagent $ABTS^{\bullet+}$ (details see below). The ABTS solution contained 1 mM ABTS (>98%, Sigma-Aldrich) and was acidified with sulfuric acid (95% w/w, Sigma-Aldrich; final concentration: 18 mM) to prevent microbial growth and to maintain a pH of 2 during the oxidation of ABTS to $ABTS^{\bullet+}$ by chlorine. The chlorine solution was prepared by diluting a concentrated hypochlorite stock solution (6–14% active chlorine, Sigma-Aldrich) in water. Free available chlorine concentrations were quantified in dilute basic solution aliquots using the molar absorptivity of hypochlorite ($\varepsilon_{292nm} = 350\ M^{-1}{\cdot}cm^{-1}$, pH 11, (Soulard et al., 1981)). To stabilize the chlorine solution, the pH was raised to 11 using a NaOH solution (1 mM). The phosphate buffer solution (500 mM phosphate; disodium hydrogen phosphate dihydrate, ≥99.5%; sodium dihydrogen phosphate monohydrate, 99.0–102.0%, Merck) was used to buffer the final reaction mixture of DOM-containing samples and the $ABTS^{\bullet+}$ reagent solution at pH 7. The ABTS, chlorine, and buffer solutions were all prepared using ultrapure water with a resistivity of >18 MΩ·cm (Arium ultrapure water system, Sartorius, Germany). Otherwise, deionized water was used (quality not monitored). All solutions were stored at room temperature in 1 L glass bottles except deionized water, which was stored in 5 L polyethylene canisters.

The stability of the ABTS and chlorine solution was ensured by monitoring the resulting $ABTS^{\bullet+}$ concentration in the final reaction mixtures of DOM-free blanks and $ABTS^{\bullet+}$ reagent solution (<1% decrease in a_{730nm} over 24 days, see Figure S1, Supporting Information (SI)). During routine operation, the EDC analyzer used approximately 24 mL ABTS solution and 10 mL chlorine solution per day. Both solutions were replaced at least every two months.

2.2. Design and operation of the EDC analyzer

The EDC analyzer automatically determined the relative residual UV absorbance and the EDC in sequential measurement cycles at a frequency of approximately one measurement per hour. At the beginning of a measurement cycle, a batch of $ABTS^{\bullet+}$ reagent solution was prepared, which was subsequently used to analyze (a) an ozonation influent, (b) a

DOM-free blank, and (c) an ozonation effluent sample. This measurement cycle was based on large parts on a previously validated procedure (Walpen et al., 2020).

Transport of all liquids (Fig. 1) was handled by a syringe pump (Cadent-3, IMI Precision) equipped with a zero-dead-volume syringe (V = 2.5 mL) connected to a 12-way rotary selector valve. The syringe pump was connected to four modules which enabled (i) preparation of an $ABTS^{\bullet+}$ reagent solution, (ii) sample collection and filtration, (iii) detection of UV absorbance and mixing, and (iv) detection of EDC. To enable the automatic operation of the EDC analyzer, all active units and sensors were connected to a programmable logic controller (PFC200, WAGO, Germany). The controller was programmed to automatically start the measurement cycles including regular cleaning intervals (see below) once the device is supplied with electrical power and was therefore able to operate autonomously. Analysis results were stored locally on a memory card and downloaded via a LTE connection to the controller.

2.2.1. *Preparation of $ABTS^{\bullet+}$ reagent solution*

To obtain a batch of $ABTS^{\bullet+}$ reagent solution (V = 2.4 mL), 1 mL of ABTS solution (1 mM), 0.35 mL of chlorine solution (1 mM) as well as 1.05 mL of water were sequentially aspirated by the syringe. The entire batch of solution was immediately dispensed to a custom-made mixing chamber (V = 3 mL, poly(methyl methacrylate)) and aspirated back into the syringe. This transfer of solution was repeated five times for complete mixing. To facilitate vertical mixing, the solution was dispensed into the mixing chamber from the top and aspirated from the bottom. The mixing resulted in a pH of 2 and the rapid oxidation ABTS to $ABTS^{\bullet+}$ by the limiting reagent chlorine (Pinkernell et al., 2000):

$$HOCl + 2ABTS + H^{+} \rightarrow Cl^{-} + 2ABTS^{\bullet+} + H_2O \quad (1)$$

Subsequently, the resulting $ABTS^{\bullet+}$ reagent solution was dispensed to the mixing chamber for temporary storage for the duration of the measurement cycle.

2.2.2. *Collection and filtration of in- and effluent of the ozonation reactor*

To minimize microbial growth in the fluidic system and potential damages by particles to moving parts of the syringe pump, sample solutions were filtered. For this purpose, sample solutions from the in- and effluent of the ozonation reactors, were each by-passed through two separate containers (V = 18 L). Two solenoid pumps (Model DLX-VFT/MBB, Etatron, Italy) continuously aspirated water from both by-pass containers through ceramic filter disks (0.45-µm pore size, Al_2O_3, 15 cm diameter, PMC model, ETL Filtration Technology, Germany) and dispensed into two separate custom-made overflow sample-collection cylinders (V = 10 mL, poly(methyl methacrylate)). The by-pass containers and the sample-collection cylinder had a hydraulic residence time of 3–5 and 7 min, respectively, based on the measured flow rate and volumes of the vessels. The filter discs, membrane pumps and sample-collection cylinders were connected with polyethylene tubing. The syringe pump was connected to the sample-collection cylinders through a three-way/two-position valve which allowed to automatically select either in- or effluent of the ozonation reactors.

2.2.3. *Detection of UV absorbance and mixing with reagent solution*

The analysis of a sample or DOM-free blank solution involved the following steps: First, the sample solution was aspirated into the syringe and partly dispensed to the photometer for the quantification of the UV absorbance at 255 nm (a_{255nm}). The fixed wavelength of the LED light source of the photometer is a negligible shift in wavelength compared to standard methods determining the UV absorbance at 254 nm. Next, the phosphate buffer solution and an aliquot of the $ABTS^{\bullet+}$ reagent solution was aspirated. The entire reaction mixture was transferred to a second mixing chamber and back for mixing. After a reaction time of 15 min, the reaction mixture was finally dispensed to the photometer for the photometric quantification of residual $ABTS^{\bullet+}$ concentration at a wavelength of 730 nm.

2.2.4. *Detection and quantification the residual a_{255nm} and EDC*

For the measurement of a_{255nm} of the DOM samples and the photometric quantification of the residual $ABTS^{\bullet+}$ concentration in the reaction mixtures at a_{730nm}, solutions were passed to a flow-through photometer (Mikron 31, RS-485 prototype, Runge, Germany) equipped with two LEDs (λ = 255 and 730 nm) as light sources and a stainless-steel flow cell with a 10-mm optical path length.

The relative residual a_{255nm} ($a_{255nm} \cdot a^{-1}_{255nm,0}$) was calculated as a_{255nm} of the ozonation effluent relative to the ozonation influent sample.

The EDC of a DOM sample was previously defined as the decrease in $ABTS^{\bullet+}$ concentration due to the reduction by DOM normalized by the DOC concentration (Walpen et al., 2020):

$$EDC = \frac{A^{blank}_{730nm} - A^{sample}_{730nm}}{\varepsilon_{ABTS^{\bullet+}} \cdot l} \cdot \frac{1}{c_{DOC}} \quad (2)$$

where A^{blank}_{730nm} and A^{sample}_{730nm} are the resulting absorbance values at 730 nm of the reaction mixtures containing the DOM-free blank and the DOM sample, respectively, $\varepsilon_{ABTS^{\bullet+}}$ is the molar absorption coefficient of $ABTS^{\bullet+}$ ($1.4 \cdot 10^4$ $M^{-1}cm^{-1}$, Scott et al., 1993; Walpen et al., 2016), l (cm) is the optical pathlength, and c_{DOC} ($mg_{DOC} \cdot L^{-1}$) is the DOC concentration in the final reaction mixture. Since DOC concentrations were

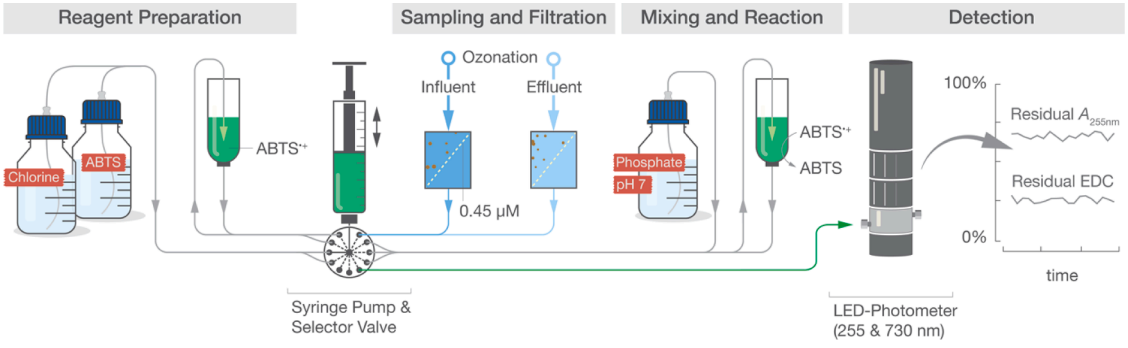

Fig. 1. Scheme of the online EDC analyzer. A syringe pump connected to a selector valve was used for liquid handling. To continuously monitor the changes in absorbance at 255 nm (a_{255nm}) and the residual electron-donating capacity (EDC) during ozonation, the analyzer sequentially executed a measurement cycle which consisted of four steps: First, an $ABTS^{\bullet+}$-reagent solution was prepared by adding chlorine solution to an ABTS-containing solution (left $ABTS^{\bullet+}$ solution). Second, a filtered sample from the influent of the ozonation reactors was aspirated by the syringe. This sample was partially dispensed to the photometer to quantify a_{255nm}. Third, the sample was mixed with an aliquot of the $ABTS^{\bullet+}$-reagent solution and mixed with the phosphate buffer (right $ABTS^{\bullet+}$ solution). Fourth, after a reaction time of 15 min, the solution was dispensed to the photometer to quantify the residual $ABTS^{\bullet+}$ concentration absorbance at 730 nm (a_{730nm}). Steps two to four were then repeated for a DOM-free blank solution and for an effluent sample.

not measured on-line, EDC values for individual samples (i.e., before or after ozonation) is reported as non-carbon-normalized EDC (EDC·c_{DOC}). However, because ozonation only marginally affects DOC concentrations (Lee et al., 2012; Nöthe et al., 2009), relative residual EDC (EDC·EDC_0^{-1}) values can be determined with the absorption coefficients at 730 nm (a_{730nm}) of the resulting reaction mixtures with the in- and effluent as well as the DOM-free blank sample:

$$EDC \cdot EDC_0^{-1} = \frac{EDC^{effluent}}{EDC^{influent}} = \frac{a_{730nm}^{blank} - a_{730nm}^{effluent}}{a_{730nm}^{blank} - a_{730nm}^{influent}} \quad (3)$$

Iron(II) species in the ozonation influent were not expected to contribute significantly to the measured EDC, because total iron concentrations were small (<20 µg·L^{-1} in ozonation-influent grab samples, Figure S2, SI) and iron(III) species were likely predominating the pool of total iron, in particular after ozonation (Løgager et al., 1992).

2.2.5. Maintenance of the EDC analyzer

The EDC analyzer required regular automated as well as manual cleaning intervals. During routine operation, the syringe pump executed a daily automated chemical cleaning and disinfection of the sample line tubing, sample mixing chamber, syringe, and photometer flow cell with diluted chlorine solution (c_{OCl^-} = 0.2 µM = 0.01 mg·L^{-1}). With this procedure bacterial growth could be avoided and no manual cleaning of the LED photometer was required. Biofilm or residues on the surfaces of the ceramic filter disks were manually removed 2–3 times per week using a brush and warm water.

2.3. Full-scale ozonation at the wastewater treatment plant of Zurich

The EDC analyzer was installed at the ozonation reactors of the municipal wastewater treatment plant Werdhölzli in Zurich, Switzerland. The treatment plant has a capacity of 670′000 person equivalents. Secondary treatment is performed in a nitrifying activated-sludge system with alternating intermittent aeration followed by clarification. Subsequently, the water is treated with O_3 for micropollutant abatement in four parallel ozonation reactors each of which had a volume of 1′535 m^3. Each reactor is divided into eight compartments by vertical flow-control baffles. Ozone-containing gas is introduced in countercurrent mode through an array of diffusers at the bottom of the first and third compartment. Finally, the ozonation effluent is passed through a sand filter for biological post-treatment before discharge to a river.

The ozonation process was monitored by measuring (i) the absorption at 254 nm (a_{254nm}) of the unfiltered in- and effluent using a flow-through spectrophotometer equipped with a flash lamp (CAS51D, Endress+Hauser, Switzerland) and (ii) the nitrite concentration in the influent using a nitrite analyzer (CA80NO, Endress+Hauser, Switzerland). For routine operation, the O_3 dose was controlled based on a combination of feed-forward (flow rate, DOC concentration estimated based on a_{254nm}, and nitrite concentration) and feed-back (relative residual a_{254nm}) control parameters. The targeted value for the relative residual a_{254nm} was 68%. This value had been obtained previously to reach a mean relative residual concentration of indicator compounds of 20% over the entire treatment plant as required by the Swiss authorities (Federal Office for the Environment, 2015).

2.3.1. Repeated sample analysis for performance assessment

To initially assess the performance of the EDC analyzer under real conditions, a batch of 500 mL was collected from both, the influent and the effluent of the ozonation reactors. Both batches were filtered (0.45-µm pore size) and then analyzed repeatedly on-site. Quantification limits (LOQ) were calculated based on the signal responses S and corresponding standard deviations σ of the analysis of DOM-free blanks (LOQ = $S_{blank} + 10 \cdot \sigma_{blank}$).

2.3.2. On-line monitoring of residual a_{255nm} and EDC

To observe the changes in a_{255nm} and EDC during ozonation on-line, the EDC analyzer monitored the common influent and effluent of two out of the four parallel ozonation reactors. The EDC analyzer had a constant sampling interval of 34 min and the hydraulic residence time of the ozonation reactor varied around a median of 29.6 min (25th and 75th percentiles were 25.3 and 38.4 min, respectively) depending on the total flow rate and the number of operating ozonation reactors. This difference between the sampling interval and the hydraulic residence time was considered negligible in comparison to the slow changes of the water quality at the in- and effluent.

2.3.3. Variation of O_3 doses in full-scale ozonation

To vary the O_3 dose during full-scale ozonation, the process control system was operated in an experimental mode based only on feed-forward control parameters (flow rate q, DOC concentration estimated based on on-line a_{254nm}, and on-line nitrite concentration) with different targeted specific O_3 doses ranging from 0.06 to 0.7 $mg_{O3} \cdot mg_{DOC}^{-1}$. The targeted O_3 doses were manually adjusted on six days in January and February of 2021 during two extended dry weather periods to minimize variations in the composition of the ozonation influent.

For selected time points, pairs of in- and effluent grab samples were collected from the sample-collection cylinders immediately after aspiration of the sample by the syringe pump of the EDC analyzer. At this point, the grab samples had already passed the ceramic filter disk and were stored at 4 °C in the dark without any further sample treatment until further laboratory analyses.

2.4. Analyses of water quality parameters of ozonation influent samples

Concentrations of DOC (LOQ = 0.5 $mg_{DOC} \cdot L^{-1}$), alkalinity (LOQ = 0.2 mM), ammonium (LOQ = 5 $\mu g_N \cdot L^{-1}$), and nitrite (LOQ = 1 $\mu g_N \cdot L^{-1}$) were quantified in all grab samples as described in section 1.3 in the SI.

2.5. Analysis of micropollutants by LC-MS

Concentrations of 22 selected micropollutants, including pharmaceuticals, X-ray contrast agents, pesticides, a food additive and a corrosion inhibitor, were quantified in the sample pairs collected from the in- and effluent of the ozonation reactor. A complete list of micropollutants and corresponding apparent second-order rate constants for the reactions with O_3 and hydroxyl radical at pH 7 is provided in Table S1 (SI). The micropollutants were selected due to their typically high abundance in WWTP effluents. Their apparent second-order rate constants for the reactions with O_3 at pH 7 covered a wide range from $5.0 \cdot 10^{-2}$ to $6.8 \cdot 10^5$ $M^{-1}s^{-1}$ (Table S1, SI). The listed apparent second-order rate constants should be considered as approximations for the pH that prevailed during the monitoring campaigns (i.e., pH = 7.6 ± 0.2). A subset of twelve micropollutants are also listed as indicator compounds for advanced wastewater treatment by the Swiss regulators (Federal Office for the Environment, 2015). Micropollutant concentrations (LOQ = 100 ng·L^{-1}) were quantified by liquid chromatography coupled to mass spectrometry (LC-MS) as detailed in section 1.5 of the SI.

2.6. Analyses of bromide, bromate, iodide and iodate by IC-MS

The O_3-reactive halogen species bromide and iodide as well as their oxidation products bromate and iodate were analyzed in the filtered grab samples by ion chromatography coupled to mass spectrometry (IC-MS). Details on the analysis are described in section 1.6 of the SI and Table S2 (SI). LOQs were 5, 1, 5, and 2.5 µg·L^{-1} for bromide, bromate, iodide and iodate, respectively, with a relative standard deviation of <10%.

2.7. Statistical modeling

Exponential regression models were fitted to the relative residual a_{255nm} and EDC as a function of specific O_3 doses by a non-linear least squares method. Logistic regression models were fitted to the relative residual micropollutant concentrations with a quasibinomial probability distribution, a logit link function and the relative residual a_{255nm} and EDC as estimators.

3. Results and discussion

3.1. Performance assessment of the EDC analyzer

The repeatability of a_{255nm} and EDC measurements was assessed by repeatedly analyzing a batch of influent and effluent of the ozonation reactors collected during routine full-scale ozonation (specific O_3 dose ~0.64 mg_{O3}•mg_C^{-1}). Measurements of a_{255nm} (Fig. 2a) were highly repeatable with mean values of 0.088 ± 0.001 cm^{-1} and 0.043 ± 0.001 cm^{-1} (mean value ± standard deviation; $n = 28$) for the in- and effluent, respectively, and were significantly above the LOQ of 0.006 cm^{-1}. Non-carbon-normalized EDC measurements (EDC·c_{DOC}) were also repeatable (Fig. 2b) with mean values for EDC·c_{DOC} of 16.2 ± 0.4 μM_{e^-} and 3.6 ± 0.3 μM_{e^-} ($n = 28$), respectively, and were also above the LOQ of 2.8 μM_{e^-}. As expected, both parameters, a_{255nm} and EDC, decreased significantly during ozonation to relative residual values of 49 ± 1% and 22 ± 2% (Fig. 2c).

The slightly larger variations of EDC values compared to a_{255nm} were due to errors introduced by the additional analytical steps required for the EDC measurement (i.e., (i) addition of reagent solutions and (ii) mixing of the resulting reaction mixture). Additional advancements and optimizations of the analyzer, specifically of the liquid handling, may further improve the precision of EDC measurements. Nevertheless, the repeatability and LOQs demonstrated that the precision of the EDC analyzer was suitable to monitor changes in a_{255nm} and EDC during routine ozonation.

3.2. On-line monitoring of a_{255nm} and EDC during full-scale ozonation

An exemplary nine-days series of on-line measurement results obtained in February 2021 with the EDC analyzer and process data from the ozonation system is shown in Fig. 3. An equivalent time series obtained in January 2021 is shown in Figure S3 (SI). Both time series were recorded to a large part under typical dry-weather conditions with high levels of nitrogen removal in the preceding nitrifying activated-sludge treatment as evidenced by the low residual ammonium concentrations of 0.5 ± 0.2 $mg_N·L^{-1}$ in the influent of the ozonation reactor. Selected water quality parameters (i.e., DOC, nitrite, and ammonium concentrations, and alkalinity, pH and conductivity) of the influent grab samples are shown in Figure S4 (SI). The consumption of O_3 by nitrite will be addressed separately below.

3.2.1. Variability of a_{255nm} and EDC•c_{DOC} in ozonation influent

In this time series (Fig. 3), a_{255nm} and EDC·c_{DOC} of the ozonation influent exhibited minor, diurnal fluctuations with stable daily average values. Values of a_{255nm} and EDC·c_{DOC} measured in the influent of the ozonation reactor ranged from 0.086 to 0.104 cm^{-1} and 17.9–22.0 μM_{e^-}, respectively. Maximum daily values of a_{255nm} and EDC·c_{DOC} were reached around midnight between 22:00 and 02:00 h. The largest relative daily increase was recorded on the second day during which a_{255nm} and EDC·c_{DOC} increased by 16% and 23%, respectively. Nitrite concentrations measured on-line ranged from 0.06 to 0.33 $mg_N·L^{-1}$ in agreement with values for similar nitrifying wastewater treatment plants (Schindler Wildhaber et al., 2015) and also followed a diurnal pattern with maximum daily values typically reached between 17:00 and 19:00. These diurnal patterns were attributed to changes in the carbon and nitrogen loads entering the activated-sludge treatment

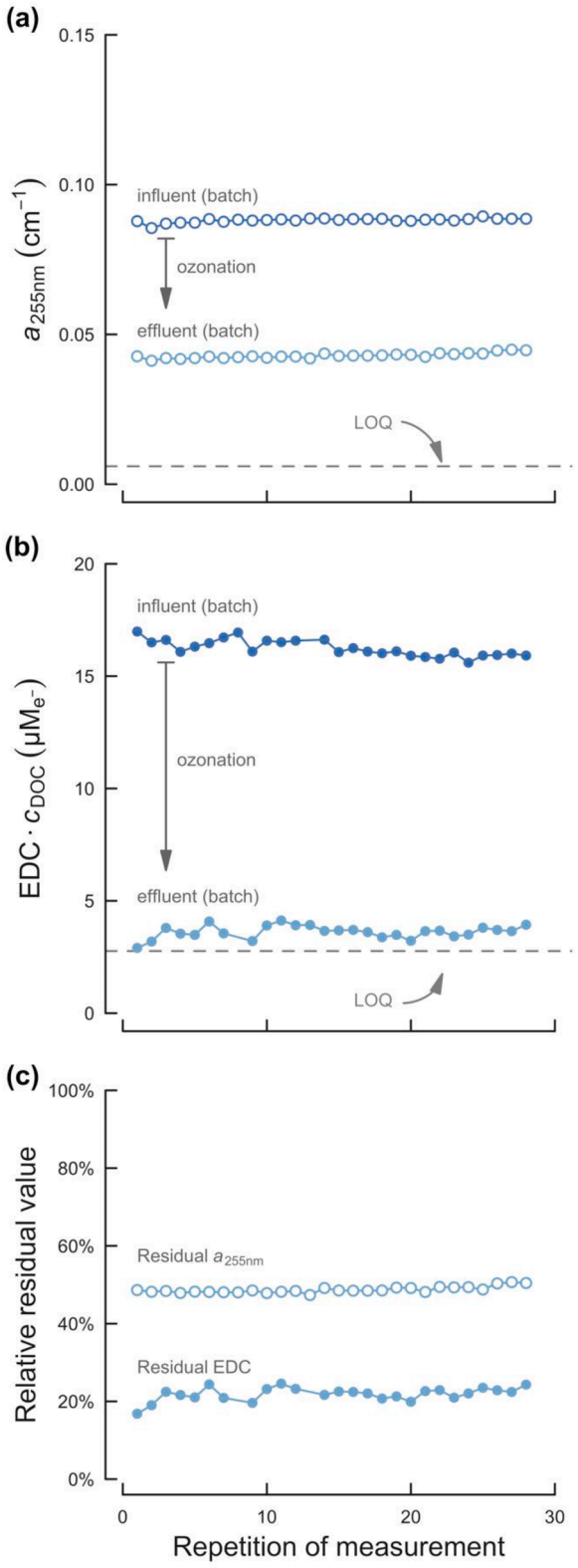

Fig. 2. Repeated measurements of a batch of influent and effluent of the ozonation reactors (specific O_3 dose ~0.64 $mg_{O3}·mg_C^{-1}$) using the EDC analyzer. (a) Absorption coefficient at 255 nm (a_{255nm}) of ozonation influent (dark circles) and effluent (light circles). (b) Non-carbon-normalized electron-donating capacity (EDC•c_{DOC}) of ozonation influent (filled dark circles) and effluent (filled light circles). (c) Relative residual a_{255nm} (open circles) and EDC (filled circles) as a result of ozonation. Limits of quantification (LOQ) are indicated by the gray dashed lines.

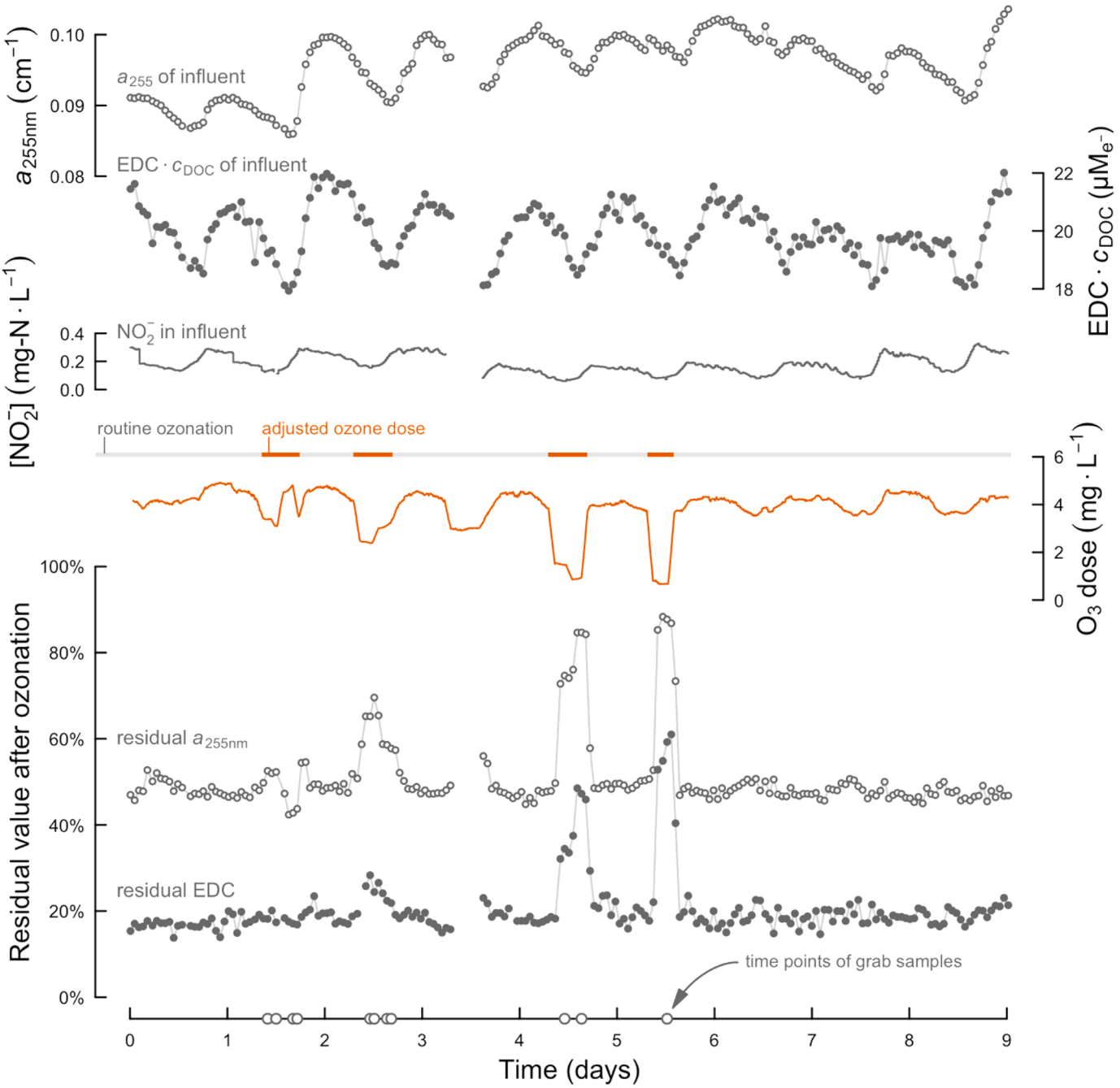

Fig. 3. Time series of a_{255nm} and EDC•c_{DOC} measured in the influent of the ozonation reactors (empty and filled circles, respectively), nitrite concentrations of the influent (gray line), O_3 dose (orange line), and residual a_{255nm} and EDC of the ozonation effluent (empty and filled circles, respectively). This time series was recorded in February 2021. The horizontal bar above the O_3 dose indicates when the specific O_3 dose was adjusted from the routine ozonation (orange lines). The empty circles on the time axis indicate the time points at which grab samples were collected for laboratory analyses. The gaps in the time series on the third day were caused by maintenances of the sampling system of the treatment plant.

basins and the effectiveness of the activated-sludge treatment. Overall, the monitored parameters indicated stable process conditions throughout this time series.

The frequency of approximately one measurement per hour was considered sufficient to capture the diurnal patterns of a_{255nm} and EDC·c_{DOC} in the ozonation influent. However, it is conceivable that these parameters may vary more rapidly under certain circumstances. For such cases, a faster measuring frequency than currently available with the EDC analyzer would be beneficial and could be achieved by shortening the reaction time or by parallel EDC measurements of the ozonation in- and effluent and the blank sample using multiple syringe pumps.

3.2.2. *Stable decrease of a_{255nm} and EDC during routine ozonation*

During routine ozonation (Fig. 3, gray horizontal bars), the treatment plant's control system maintained a constant decrease in the UV absorption of the unfiltered in- and effluent of the ozonation reactors. This resulted in O_3 doses of 2.9–4.9 $mg_{O3}·L^{-1}$ during the monitored time series (Fig. 3, orange line during routine ozonation). The primary driver for the variations in the O_3 dose was the changes in nitrite concentrations in the ozonation influent. Because nitrite readily reacts with O_3 via an O-transfer reaction forming nitrate (Hoigné et al., 1985; Naumov

et al., 2010), the nitrite measured in the influent accounted for 7–43% of the O_3 dose. Ozonation resulted in a significant and stable decreases in both, a_{255nm} and EDC, independent of the water quality fluctuations in the influent. The mean residual value of a_{255nm} decreased to 48 ± 3%, while the mean residual value of EDC decreased to 19 ± 3%. These small relative standard deviations illustrate the reliability of the measurements obtained with the EDC analyzer.

3.3. Variations of O_3 doses during full-scale ozonation

To investigate the effects of changes in the specific O_3 dose on a_{255nm} and EDC during full-scale ozonation, the feed-back control system was temporarily disabled and targeted specific O_3 doses were varied using only the feed-forward control (Fig. 3, orange horizontal bars). This resulted in O_3 doses of 0.7–4.8 $mg_{O3}{\cdot}L^{-1}$. Similar experiments were conducted on two more days (time series data shown in Figure S3, SI). Generally, these O_3 doses were lower compared to the doses, which would have been applied during routine operation except on the second day of the time series when slightly higher O_3 doses were reached.

3.3.1. Responses of residual a_{255nm} and EDC to lower O_3 doses

The lower O_3 doses resulted in higher residual a_{255nm} and EDC in comparison to routine ozonation with maximum values of 88% and 61%, respectively (Fig. 3). The slightly higher O_3 doses on the second day only resulted in an additional decrease in the residual a_{255nm} but did not appear to affect residual EDC values.

The time points at which grab samples were collected from the in- and effluent of the ozonation reactors are indicated on the time axis in Fig. 3 (circles). The corresponding residual a_{255nm} and EDC values (circles in Fig. 4b) spanned the entire range observed for both parameters during the monitoring campaign.

3.3.2. Consumption of O_3 by nitrite and iodide

Laboratory analyses of anions in- and effluent grab samples indicated that nitrite and iodide competed with DOM for O_3. Nitrite concentrations ranged from 0.09 to 0.55 mg-N·L^{-1} in the influent samples (Figure S5a, SI). Residual nitrite concentrations relative to the corresponding influent concentrations decreased proportionally to the applied O_3 doses (Figure S5b, SI) in agreement with the fast oxidation of nitrite to nitrate by O_3 with $k_{NO_2^-} = 5.83{\cdot}10^5\ M^{-1}s^{-1}$ (Liu et al., 2001). Iodide was present at unexpectedly high concentrations in a subset of influent grab samples. While iodide concentrations in the influent samples ranged between 2.6 and 11.0 µg·L^{-1} on January 11–13, they ranged between 31.3 and 547 µg·L^{-1} on February 22–26 (Figure S5c, SI), exceeding the expected range for municipal wastewater (Gong et al., 2018) by approximately one order of magnitude. The source of those large iodine loads remained unclear. As iodide is rapidly oxidized by O_3 forming iodate (Bichsel and von Gunten, 1999), iodate formation also increased proportionally with increasing applied O_3 doses (Figure S5d, SI). For all time points, the mean mass balance of iodide and iodate concentration from in- to effluent (i.e., $(c_{I^-}^{effl.} + c_{IO_3^-}^{effl.})/(c_{I^-}^{infl.} + c_{IO_3^-}^{infl.})$) was 102 ± 20% (Figure S5e, SI), indicating that O_3 oxidized a fraction of iodide completely to iodate. Because of this significant consumption of O_3 by nitrite and iodide, both oxidation reactions were accounted for in the calculation of specific O_3 doses (see below).

3.3.3. Decreases in a_{255nm} and EDC during ozonation

The variations in O_3 doses allowed to monitor changes in a_{255nm} and EDC as a function of the specific O_3 dose. In the grab samples, specific O_3 doses, which were calculated by carbon-normalizing O_3 doses and correcting for nitrite consumption ($\Delta[O_3]/\Delta[NO_2^-] \approx 1$) as well as iodate formation ($\Delta[O_3]/\Delta[IO_3^-] \approx -3$), ranged from 0.13 to 0.91 $mg_{O3}{\cdot}mg_{DOC}^{-1}$. Along this range, the relative residual a_{255nm} and EDC decreased exponentially with increasing specific O_3 dose (Fig. 4**a**). Residual values of a_{255nm} decreased relatively uniformly to 42% at the highest specific O_3 dose. In comparison, relative residual EDC values showed a steeper decrease to 29% for specific O_3 doses up to 0.34 $mg_{O3}{\cdot}mg_C^{-1}$ (model estimate) and plateaued towards higher ozone doses. Between 0.5 $mg_{O3}{\cdot}mg_{DOC}^{-1}$ and the highest specific O_3 dose of 0.91 $mg_{O3}{\cdot}mg_{DOC}^{-1}$, the relative residual EDC only further decreased from 22 to 17%. Therefore, the current analytical method may not be sufficiently sensitive for O_3 doses >0.5 $mg_{O3}{\cdot}mg_C^{-1}$ using EDC as control parameter. However, the high sensitivity of EDC towards small specific O_3 doses implies that the EDC is suited for treatment processes applying low specific O_3 doses <0.5 $mg_{O3}{\cdot}mg_C^{-1}$, such as a combination of ozonation with activated-carbon adsorption (Müller et al., 2019; Reungoat et al., 2012).

The fact that the data for both parameters each consistently followed the same exponential trend despite being obtained on six days distributed over two months (i.e., January 5 to March 3, 2021) suggests a high repeatability even over long periods of time. Moreover, two time points

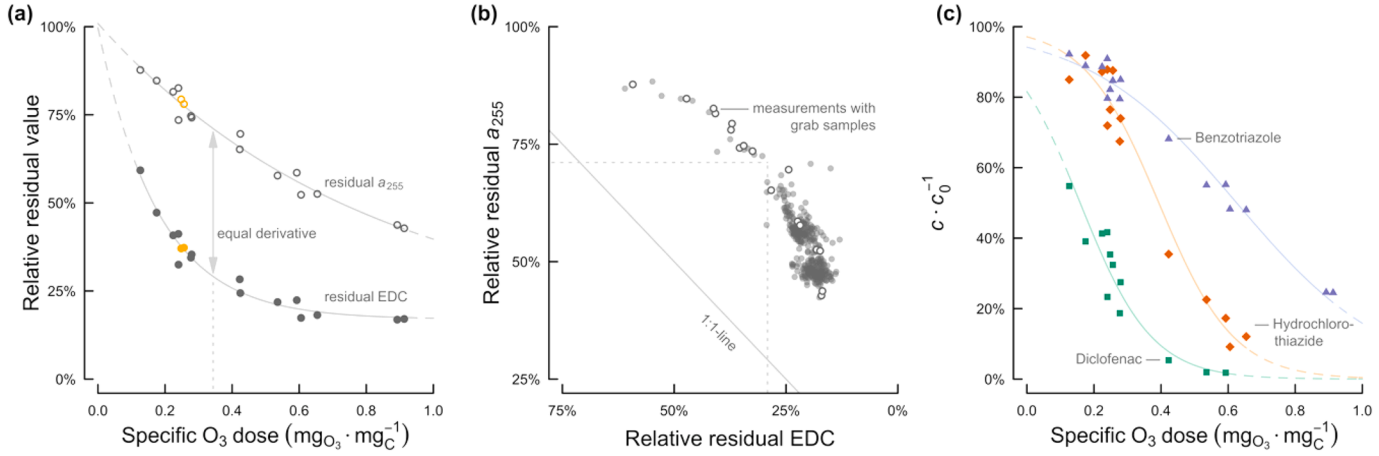

Fig. 4. (a) Relative residual a_{255nm} (empty circles) and relative residual EDC (filled circles) as a function of the specific O_3 dose. The specific O_3 dose was corrected for nitrite consumption and iodate formation during ozonation. Exponential models were fitted to the data by a non-linear least-squares method (solid lines; extrapolations indicated by dashed lines). The values of the derivation for both models were the same at a specific ozone dose of 0.34 $mg_{O3}{\cdot}mg_C^{-1}$ (vertical arrow). Two time points were collected outside typical dry-weather conditions (yellow symbols). (b) Relative residual a_{255nm} as a function of the relative residual EDC. This data was re-plotted from the time series in Fig. 3. The measurements for which grab samples were collected are indicated by the empty circles. The value of relative residual a_{255nm} and EDC corresponding to a specific ozone dose of 0.34 $mg_{O3}{\cdot}mg_C^{-1}$ is indicated by the dotted horizontal and vertical lines, respectively. (c) Relative residual concentrations of selected micropollutants measured in the grab samples as a function of the specific O_3 dose. Logistic regression models were fitted to the data with the specific O_3 dose as explanatory variable (solid lines; extrapolations indicated by dashed lines).

were collected outside typical dry-weather conditions (Figure S3, SI) and do not appear to deviate from the observed trends either (indicated by yellow symbols in Fig. 4a), indicating robust responses of both parameters also during different operational conditions.

The decreases in a_{255nm} and EDC after full-scale ozonation were both compared to results obtained previously in laboratory ozonation experiments for different secondary-treated wastewater effluents (Chon et al., 2015; Önnby et al., 2018; Walpen et al., 2020). As expected, the relative residual values of a_{255nm} measured in this study were in good agreement with previous results (Figure S6, SI). In contrast, relative residual EDC values only agreed for specific O_3 doses up to ~0.25 $mg_{O3}{\cdot}mg_C^{-1}$ and then approached different end points for higher doses (Figure S6, SI). More specifically, relative residual EDC values found in this study and by Önnby et al. (2018) reached lower end points compared to values reported in Chon et al. (2015) and Walpen et al. (2020). The different trends likely originated from differences in (i) the chemical composition of secondary-treated wastewater effluents or (ii) the analytical conditions used for the operationally-defined quantification of EDC of DOM. The first hypothesis is supported by the fact that relative residual EDC values in this study are lower than reported in Walpen et al. (2020) despite the application of the same analytical conditions. In addition, the same source of sample was used in these two studies, which further implies that storage time and conditions affect the EDC of DOM. Overall, these results confirm that changes in a_{254nm} in laboratory ozonation experiments are representative for full-scale systems, yet a similar comparison for EDC remains inconclusive and requires a systematic assessment.

3.3.4. Correlation between residual a_{255nm} and EDC during ozonation

To directly compare the responses of both parameters, the relative residual a_{255nm} was replotted as a function of the relative residual EDC (Fig. 4b). The trajectory of these data pairs collected over a time span of two months (i.e., January 5 to March 3, 2021) were correlated non-linearly. For relative residual EDC values >29% and relative residual a_{255nm} >71% (i.e., for specific ozone doses <0.34 $mg_{O3}{\cdot}mg_C^{-1}$), the relative decrease in EDC was more pronounced compared to the decrease in a_{255nm}. This trend was inversed towards lower relative residual values of a_{255nm} and EDC, respectively. The absence of significant deviations from this correlation suggests a consistent response of a_{255nm} and EDC to ozonation for at least several weeks, indicating a high degree of redundancy among the two parameters for a potential on-line estimation of micropollutant abatement. Yet, it is conceivable that changes in the chemical composition affecting either the UV absorbance or redox properties of the ozonation influent, for example due to a contamination, could result in irregular responses causing deviations from the observed trend. In such a case, the availability of two control parameters may facilitate the identification of such atypical process conditions.

3.3.5. Micropollutant abatement during ozonation

Concentrations of the 22 micropollutants determined in the in- and effluent of the ozonation reactors are summarized in Figure S7 (SI). Median influent concentrations of 19 micropollutants exceeded the quantification limit of 100 $ng{\cdot}L^{-1}$. The highest median influent concentrations were measured for benzotriazole (3.7 $\mu g{\cdot}L^{-1}$), iomeprol (2.7 $\mu g{\cdot}L^{-1}$), diatrizoate (2.4 $\mu g{\cdot}L^{-1}$), diclofenac (1.7 $\mu g{\cdot}L^{-1}$), and gabapentin (1.5 $\mu g{\cdot}L^{-1}$).

As expected, all sample pairs generally contained lower concentrations of micropollutants in the effluent than in the influent sample. Residual micropollutant concentrations are shown exemplary for diclofenac ($k_{app,O3} = 6.8{\cdot}10^5$ $M^{-1}s^{-1}$), hydrochlorothiazide ($k_{app,O3} = 8.5{\cdot}10^4$ $M^{-1}s^{-1}$), and benzotriazole ($k_{app,O3} = 35$ $M^{-1}s^{-1}$) as a function of specific O_3 dose (Fig. 4c, shown for all 22 micropollutants in Figure S8, SI). Residual concentrations decreased proportionally to increasing specific O_3 doses for all micropollutants except for the pesticide diuron and the metabolite *N*-(4)-acetylsulfamethoxazole. For these two compounds no meaningful correlation was obtained because their concentrations were below the quantification limit in most samples.

Overall, the extent of abatement was correlated to the second-order rate constants of the reactions of these compounds with O_3 (Figure S9, SI). This observation is consistent with the presence of both, ozone and hydroxyl radical as oxidants during the ozonation process (Bourgin et al., 2017; Hollender et al., 2009; Lee et al., 2013). While the observed micropollutants had a similar reactivity towards hydroxyl radicals, their second-order rate constants for the reaction with ozone ranged over eight orders of magnitude (Table S1, SI), which resulted in a more pronounced abatement of micropollutants with high ozone reactivity.

The extent of micropollutant abatement was comparable to previous reports from similar full-scale ozonation systems (Bourgin et al., 2018; Hollender et al., 2009). The relative residual micropollutant concentrations observed in this study were generally slightly higher at the same specific O_3 dose (Figure S8, SI) implying marginally lower oxidant exposures in the ozonation reactors at the wastewater treatment plant in Zurich for the same specific O_3 dose.

3.3.6. Estimation of micropollutant abatement based on a_{255nm} and EDC

The relative residual concentrations of diclofenac, hydrochlorothiazide, and benzotriazole were re-plotted as a function of the relative residual a_{255nm} (Fig. 5a) and EDC (Fig. 5b). The relative residual concentrations of these three micropollutants decreased non-linearly with the decrease of both parameters. Similar trends were also observed for the remaining set of micropollutants (Figures S10 and S11, SI), except for Diuron and *N*-(4)-acetylsulfamethoxazole due to the limited data as described above.

For each of the 22 analyzed micropollutants, a logistic regression model was fitted to the relative residual concentrations with either the relative residual a_{255nm} or EDC as explanatory variable. The fitted models are shown as solid lines in Figs. 5a and 5b for diclofenac, hydrochlorothiazide, and benzotriazole as well as in Figures S10 and S11 (SI) for the remaining set of micropollutants.

To compare the performance of both explanatory variables, the quality of the regression models was summarized in a separate plot for both explanatory variables. In Fig. 5c, all observed relative residual concentrations for all micropollutants were plotted as a function of the corresponding value estimated using relative residual a_{255nm} as explanatory variable. The same plot is shown in Fig. 5d for the relative residual EDC as explanatory variable. The closer the cloud of data points are to the 1:1-line, the smaller are the residuals of the fitted models. Both explanatory variables, the relative residual a_{255nm} and EDC, allowed to appropriately estimate the relative residual micropollutant concentration. The estimated values show a slightly larger spread to the observed values if the relative residual EDC is used (fitted linear regression model has $R^2 = 0.92$, Fig. 5c) compared to the relative residual a_{255nm} ($R^2 = 0.97$, Fig. 5d). This larger spread originated from the larger relative standard deviations of the EDC compared to a_{255nm}. However, as described above, instrumental improvements may further increase the precision of the method. Taken together, the logistic regression models allowed to independently estimate micropollutant abatement based on either of the two monitored parameters measured on-line.

3.3.7. Derivation of target values for the residual a_{255nm} and EDC

Based on the fitted logistic regression models, target values of the relative residual a_{255nm} and EDC could be derived for any arbitrary micropollutant abatement target. To demonstrate this, the micropollutant abatement was quantified according to the Swiss regulatory framework by averaging the abatement of twelve indicator compounds (see Table S1, SI). Therefore, the models fitted to the relative residual concentration of the twelve indicator compounds were selected (shown as light lines in Figs. 5e and f) and averaged along the explanatory variables (shown as bold line in Figs. 5e and f). Based on these model averages, a micropollutant abatement target of e.g. 75% (i.e., an average relative residual micropollutant concentration of 25%) would

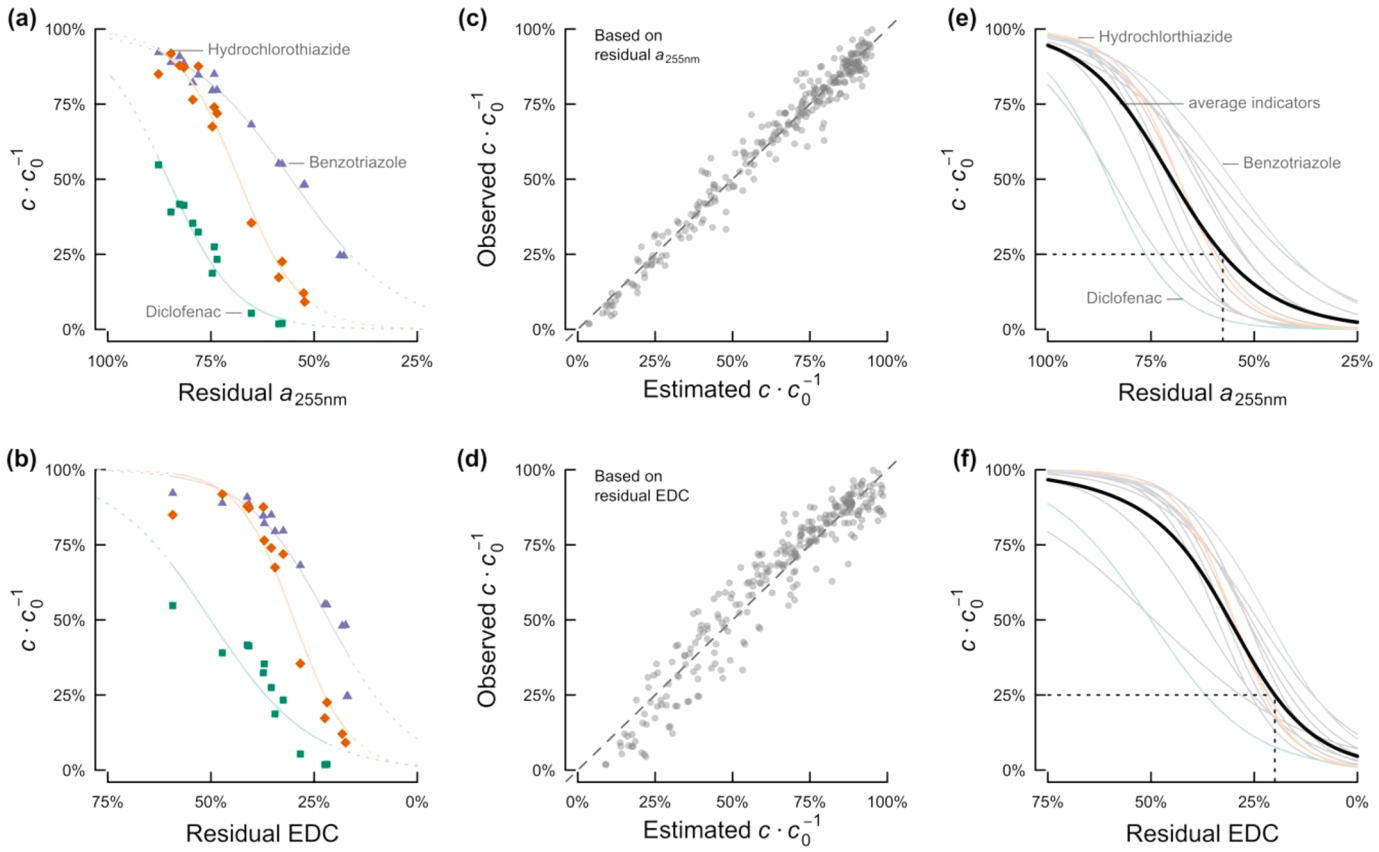

Fig. 5. Relative residual concentrations of selected micropollutants measured in the grab samples as a function of (a) the relative residual a_{255nm} and (b) the relative residual EDC. Logistic regression models were fitted to the data with the relative residual a_{255nm} and EDC as explanatory variable (solid lines; extrapolations indicated by dashed lines). The observed residual micropollutant concentrations for all 22 analyzed micropollutants versus the estimated residual concentrations using (c) the relative residual a_{255nm} and (d) the relative residual EDC as estimator. Models (light lines) which were fitted to the relative residual concentrations of the 12 indicator compounds specified by the Swiss regulator with (e) relative residual a_{255nm} and (f) relative residual EDC as explanatory variable. These 12 fitted models were averaged along the explanatory variable (bold lines). An average micropollutant abatement of 75% and the corresponding relative residual a_{255nm} and EDC are indicated by the dotted lines.

correspond to a relative residual a_{255nm} of 57% and a relative residual EDC of 19%, respectively (dotted lines in Figs. 5e and f). In a practical application, these target values for the relative residual a_{255nm} and EDC could directly be applied in a feed-back control system for the ozonation of secondary-treated wastewater. However, as noted above, the limited sensitivity of the EDC as control parameter needs to be taken into account for O_3 doses >0.5 $mg_{O3} \cdot mg_C^{-1}$.

3.3.8. *Assessment of bromate formation based on a_{255nm} and EDC*

Concentrations of bromide in the influent samples ranged from 124 to 807 $\mu g \cdot L^{-1}$ (Figure S12a, SI), indicating significant temporal variations in the load of bromide in the influent of the wastewater treatment plant. Ozonation resulted in the formation of the potentially carcinogenic oxidation by-product bromate which was present at concentrations from <1.0 to 7.8 $\mu g \cdot L^{-1}$ in the effluent samples (Figure S12b, SI). The molar conversion of bromide to bromate was proportional to the specific O_3 dose (Figure S12c, SI) and increased exponentially to 2.1% at the highest specific O_3 dose of 0.91 $mg_{O3} \cdot mg_C^{-1}$, both of which is consistent with previous studies (Bourgin et al., 2018; Soltermann et al., 2016). Molar conversion of bromide to bromate increased significantly to values >1% when the relative residual values of a_{255nm} and EDC fell below a threshold of 49% and 18%, respectively (Figures S12d and e, SI). These threshold values may therefore help to identify ozonation conditions with relative bromide conversion of more than 1%, however, the relative residual EDC is close to its observed end point value of 17% (see above). In addition, these parameters are not suited to assess absolute bromate concentrations in ozonation effluents, since its formation during ozonation is proportional to the bromide influent concentration and only absolute bromate concentrations are relevant for regulators.

4. Conclusions

In this study an automated, on-line EDC analyzer was used to continuously monitor the relative changes in a_{255nm} and EDC during full-scale ozonation of a secondary-treated municipal wastewater. Variations of the specific O_3 doses allowed to assess the responses in a_{255nm} and EDC and their correlation with micropollutant abatement and bromate formation. Based on the results, the following conclusions can be drawn:

- During a multi-week monitoring campaign with varying O_3 doses, responses in residual a_{255nm} and EDC were correlated but non-linearly. This finding suggests, that expanding existing absorbance-based ozonation control-framework by integrating EDC as feedback-control parameters could offer (i) robustness through the application of a second, independent surrogate parameter to assess micropollutant abatement and (ii) additional options to detect problems in the process control.
- Relative residual values of a_{255nm} and EDC both decreased exponentially with increasing specific O_3 doses. In comparison to relative residual a_{255nm}, the relative residual EDC responded more sensitive to increases in specific O_3 doses <0.34 $mg_{O3} \cdot mg_C^{-1}$, whereas an opposite trend was observed for higher specific ozone doses. This finding implies that monitoring residual EDC in addition to a_{255nm}

may be particularly interesting for low O_3 dose applications such as combinations of ozonation and activated-carbon adsorption for enhanced wastewater treatment.

- For 20 out of 22 selected micropollutants, relative residual concentrations decreased proportionally to increasing specific O_3 doses and thus also to relative residual a_{255nm} and EDC. The fitted logistic regression models allowed to derive target values of relative residual a_{255nm} and EDC for specific micropollutant abatement targets.
- Bromate concentrations in the effluent of the ozonation reactors cannot be predicted by decreases in UV absorption or EDC during ozonation because they also depend on the bromide concentrations in the influent. However, both parameters are suitable to identify ozonation conditions with elevated conversions of bromide to bromate.

Declaration of Competing Interest

The authors declare that they have no known competing financial interests or personal relationships that could have appeared to influence the work reported in this paper.

Acknowledgments

We thank Elisabeth Muck, Joanna Houska, Marc Böhler, Richard Fankhauser, Christian Ebi, Julie Tolu, Andreas Raffainer, and Seba Soldo (all Eawag) for supporting the development of the EDC analyzer and for laboratory analyses. We further thank the staff at the Werdhölzli wastewater treatment plant Christian Abegglen, Nina Gubser, Rey Eyer, and David Kaulbach (all Entsorgung + Recycling Zürich) for enabling the monitoring campaign at the full-scale ozonation reactors. Finally, we thank the Swiss Federal Office for the Environment (FOEN, Project No R182–0749) for funding this project.

Supplementary materials

Supplementary material associated with this article can be found, in the online version, at doi:10.1016/j.watres.2021.117858.

References

Aeschbacher, M., Graf, C., Schwarzenbach, R.P., Sander, M., 2012. Antioxidant properties of humic substances. Environ. Sci. Technol. 46, 4916–4925.
Aeschbacher, M., Sander, M., Schwarzenbach, R.P., 2010. Novel Electrochemical Approach to Assess the Redox Properties of Humic Substances. Environ. Sci. Technol. 44, 87–93.
Bahr, C., Schumacher, J., Ernst, M., Luck, F., Heinzmann, B., Jekel, M., 2007. SUVA as control parameter for the effective ozonation of organic pollutants in secondary effluent. Water Sci. Technol. 55, 267–274.
Bichsel, Y., von Gunten, U., 1999. Oxidation of Iodide and Hypoiodous Acid in the Disinfection of Natural Waters. Environ. Sci. Technol. 33, 4040–4045.
Bourgin, M., Beck, B., Boehler, M., Borowska, E., Fleiner, J., Salhi, E., Teichler, R., von Gunten, U., Siegrist, H., McArdell, C.S., 2018. Evaluation of a full-scale wastewater treatment plant upgraded with ozonation and biological post-treatments: abatement of micropollutants, formation of transformation products and oxidation by-products. Water Res 129, 486–498.
Bourgin, M., Borowska, E., Helbing, J., Hollender, J., Kaiser, H.-P., Kienle, C., McArdell, C.S., Simon, E., von Gunten, U., 2017. Effect of operational and water quality parameters on conventional ozonation and the advanced oxidation process O3/H2O2: kinetics of micropollutant abatement, transformation product and bromate formation in a surface water. Water Res 122, 234–245.
Buffle, M.-O., Schumacher, J., Meylan, S., Jekel, M., von Gunten, U., 2006a. Ozonation and Advanced Oxidation of Wastewater: effect of O_3 Dose, pH, DOM and $HO^{\bullet}$-Scavengers on Ozone Decomposition and $HO^{\bullet}$ Generation. Ozone Sci. Eng. 28, 247–259.
Buffle, M.-O., Schumacher, J., Salhi, E., Jekel, M., von Gunten, U., 2006b. Measurement of the initial phase of ozone decomposition in water and wastewater by means of a continuous quench-flow system: application to disinfection and pharmaceutical oxidation. Water Res 40, 1884–1894.
Buffle, M.-O., von Gunten, U., 2006. Phenols and Amine Induced $HO^{\bullet}$ Generation During the Initial Phase of Natural Water Ozonation. Environ. Sci. Technol. 40, 3057–3063.
Chon, K., Salhi, E., von Gunten, U., 2015. Combination of UV absorbance and electron donating capacity to assess degradation of micropollutants and formation of bromate during ozonation of wastewater effluents. Water Res 81, 388–397.
Chys, M., T, M., Audenaert, W., Deniere, E., Thérèse, F.C., Mortier, S., Van Langenhove, H., Nopens, I., Demeestere, K., W, H., Van Hulle, S., 2017. Surrogate-Based Correlation Models in View of Real-Time Control of Ozonation of Secondary Treated Municipal Wastewater—Model Development and Dynamic Validation. Environ. Sci. Technol. 51, 14233–14243.
Deniere, E., Chys, M., Audenaert, W., Nopens, I., Van Langenhove, H., Van Hulle, S., Demeestere, K., 2021. Status and needs for online control of tertiary ozone-based water treatment: use of surrogate correlation models for removal of trace organic contaminants. Rev. Environ. Sci. Bio/Technol. 1–35.
Dickenson, E.R.V., Drewes, J.E., Sedlak, D.L., Wert, E.C., Snyder, S.A., 2009. Applying Surrogates and Indicators to Assess Removal Efficiency of Trace Organic Chemicals during Chemical Oxidation of Wastewaters. Environ. Sci. Technol. 43, 6242–6247.
Eggen, R.I.L., Hollender, J., Joss, A., Schärer, M., Stamm, C., 2014. Reducing the Discharge of Micropollutants in the Aquatic Environment: the Benefits of Upgrading Wastewater Treatment Plants. Environ. Sci. Technol. 48, 7683–7689.
Federal Office for the Environment, 2015. Erläuternder Bericht zur Änderung der Gewässerschutzverordnung (Explanatory Report on the Changes to the Swiss Federal Water Protection Ordinance), M473–0796.
Gerrity, D., Gamage, S., Jones, D., Korshin, G.V., Lee, Y., Pisarenko, A., Trenholm, R.A., von Gunten, U., Wert, E.C., Snyder, S.A., 2012. Development of surrogate correlation models to predict trace organic contaminant oxidation and microbial inactivation during ozonation. Water Res 46, 6257–6272.
Gong, T., Zhang, X., Liu, W., Lv, Y., Han, J., Choi, K.C., Li, W., Xian, Q., 2018. Tracing the sources of iodine species in a non-saline wastewater. Chemosphere 205, 643–648.
Hoigné, J., Bader, H., Haag, W.R., Staehelin, J., 1985. Rate constants of reactions of ozone with organic and inorganic compounds in water-III. Inorganic compounds and radicals. Water Res 19, 993–1004.
Hollender, J., Zimmermann, S.G., Koepke, S., Krauss, M., McArdell, C.S., Ort, C., Singer, H., von Gunten, U., Siegrist, H., 2009. Elimination of Organic Micropollutants in a Municipal Wastewater Treatment Plant Upgraded with a Full-Scale Post-Ozonation Followed by Sand Filtration. Environ. Sci. Technol. 43, 7862–7869.
Katsoyiannis, I.A., Canonica, S., von Gunten, U., 2011. Efficiency and energy requirements for the transformation of organic micropollutants by ozone, O_3/H_2O_2 and UV/H_2O_2. Water Res 45, 3811–3822.
Lee, C.O., Howe, K.J., Thomson, B.M., 2012. Ozone and biofiltration as an alternative to reverse osmosis for removing PPCPs and micropollutants from treated wastewater. Water Res 46, 1005–1014.
Lee, Y., Gerrity, D., Lee, M., Encinas Bogeat, A., Salhi, E., Gamage, S., Trenholm, R.A., Wert, E.C., Snyder, S.A., von Gunten, U., 2013. Prediction of Micropollutant Elimination during Ozonation of Municipal Wastewater Effluents: use of Kinetic and Water Specific Information. Environ. Sci. Technol. 47, 5872–5881.
Lee, Y., von Gunten, U., 2010. Oxidative transformation of micropollutants during municipal wastewater treatment: comparison of kinetic aspects of selective (chlorine, chlorine dioxide, ferrateVI, and ozone) and non-selective oxidants (hydroxyl radical). Water Res 44, 555–566.
Liu, Q., Schurter, L.M., Muller, C.E., Aloisio, S., Francisco, J.S., Margerum, D.W., 2001. Kinetics and Mechanisms of Aqueous Ozone Reactions with Bromide, Sulfite, Hydrogen Sulfite, Iodide, and Nitrite Ions. Inorg. Chem. 40, 4436–4442.
Løgager, T., Holcman, J., Sehested, K., Pedersen, T., 1992. Oxidation of ferrous ions by ozone in acidic solutions. Inorg. Chem. 31, 3523–3529.
Müller, J., Drewes, J.E., Hübner, U., 2019. Investigating synergies in sequential biofiltration-based hybrid systems for the enhanced removal of trace organic chemicals from wastewater treatment plant effluents. Environ. Sci. Water Res. Technol. 5, 1423–1435.
Nanaboina, V., Korshin, G.V., 2010. Evolution of Absorbance Spectra of Ozonated Wastewater and Its Relationship with the Degradation of Trace-Level Organic Species. Environ. Sci. Technol. 44, 6130–6137.
Naumov, S., Mark, G., Jarocki, A., von Sonntag, C., 2010. The Reactions of Nitrite Ion with Ozone in Aqueous Solution – New Experimental Data and Quantum-Chemical Considerations. Ozone Sci. Eng. 32, 430–434.
Nöthe, T., Fahlenkamp, H., von Sonntag, C., 2009. Ozonation of Wastewater: rate of Ozone Consumption and Hydroxyl Radical Yield. Environ. Sci. Technol. 43, 5990–5995.
Önnby, L., Walpen, N., Salhi, E., Sander, M., von Gunten, U., 2018. Two analytical approaches quantifying the electron donating capacities of dissolved organic matter to monitor its oxidation during chlorination and ozonation. Water Res 144, 677–689.
Pinkernell, U., Nowack, B., Gallard, H., von Gunten, U., 2000. Methods for the photometric determination of reactive bromine and chlorine species with ABTS. Water Res 34, 4343–4350.
Ramseier, M.K., von Gunten, U., 2009. Mechanisms of Phenol Ozonation—Kinetics of Formation of Primary and Secondary Reaction Products. Ozone Sci. Eng. 31, 201–215.
Remucal, C.K., Salhi, E., Walpen, N., von Gunten, U., 2020. Molecular-Level Transformation of Dissolved Organic Matter during Oxidation by Ozone and Hydroxyl Radical. Environ. Sci. Technol. 54, 10351–10360.
Reungoat, J., Escher, B.I., Macova, M., Argaud, F.X., Gernjak, W., Keller, J., 2012. Ozonation and biological activated carbon filtration of wastewater treatment plant effluents. Water Res 46, 863–872.
Schindler Wildhaber, Y., Mestankova, H., Schärer, M., Schirmer, K., Salhi, E., von Gunten, U., 2015. Novel test procedure to evaluate the treatability of wastewater with ozone. Water Res 75, 324–335.
Scott, S.L., Chen, W.J., Bakac, A., Espenson, J.H., 1993. Spectroscopic parameters, electrode potentials, acid ionization constants, and electron exchange rates of the 2,2'-azinobis(3-ethylbenzothiazoline-6-sulfonate) radicals and ions. J. Phys. Chem. 97, 6710–6714.

Soltermann, F., Abegglen, C., Götz, C., von Gunten, U., 2016. Bromide Sources and Loads in Swiss Surface Waters and Their Relevance for Bromate Formation during Wastewater Ozonation. Environ. Sci. Technol. 50, 9825–9834.
Song, Z.M., Xu, Y.L., Liang, J.K., Peng, L., Zhang, X.Y., Du, Y., Lu, Y., Li, X.Z., Wu, Q.Y., Guan, Y.T., 2021. Surrogates for on-line monitoring of the attenuation of trace organic contaminants during advanced oxidation processes for water reuse. Water Res.
Soulard, M., Bloc, F., Hatterer, A., 1981. Diagrams of Existence of Chloramines and Bromamines in Aqueous Solution. J. Chem. Soc. Dalt. Trans. 2300–2310.
Stapf, M., Miehe, U., Jekel, M., 2016. Application of online UV absorption measurements for ozone process control in secondary effluent with variable nitrite concentration. Water Res 104, 111–118.
Tentscher, P.R., Bourgin, M., von Gunten, U., 2018. Ozonation of Para-Substituted Phenolic Compounds Yields p-Benzoquinones, Other Cyclic α,β-Unsaturated Ketones, and Substituted Catechols. Environ. Sci. Technol. 52, 4763–4773.
Völker, J., Stapf, M., Miehe, U., Wagner, M., 2019. Systematic Review of Toxicity Removal by Advanced Wastewater Treatment Technologies via Ozonation and Activated Carbon. Environ. Sci. Technol. 53, 7215–7233.
von Gunten, U., 2018. Oxidation Processes in Water Treatment: are We on Track? Environ. Sci. Technol. 52, 5062–5075.
von Gunten, U., Hoigné, J., 1994. Bromate Formation during Ozonization of Bromide-Containing Waters: interaction of Ozone and Hydroxyl Radical Reactions. Environ. Sci. Technol. 28, 1234–1242.
von Sonntag, C., von Gunten, U., 2012. Chemistry of Ozone in Water and Wastewater Treatment: From Basic Principles to Applications. IWA Publishing, London.
Walpen, N., Houska, J., Salhi, E., Sander, M., von Gunten, U., 2020. Quantification of the electron donating capacity and UV absorbance of dissolved organic matter during ozonation of secondary wastewater effluent by an assay and an automated analyzer. Water Res 185, 116235.
Walpen, N., Schroth, M.H., Sander, M., 2016. Quantification of Phenolic Antioxidant Moieties in Dissolved Organic Matter by Flow-Injection Analysis with Electrochemical Detection. Environ. Sci. Technol. 50, 6423–6432.
Wenk, J., Aeschbacher, M., Salhi, E., Canonica, S., von Gunten, U., Sander, M., 2013. Chemical Oxidation of Dissolved Organic Matter by Chlorine Dioxide, Chlorine, And Ozone: effects on Its Optical and Antioxidant Properties. Environ. Sci. Technol. 47, 11147–11156.
Wert, E.C., Rosario-Ortiz, F.L., Snyder, S.A., 2009a. Effect of ozone exposure on the oxidation of trace organic contaminants in wastewater. Water Res 43, 1005–1014.
Wert, E.C., Rosario-Ortiz, F.L., Snyder, S.A., 2009b. Using Ultraviolet Absorbance and Color To Assess Pharmaceutical Oxidation during Ozonation of Wastewater. Environ. Sci. Technol. 43, 4858–4863.
Westerhoff, P., Aiken, G., Amy, G., Debroux, J., 1999. Relationships between the structure of natural organic matter and its reactivity towards molecular ozone and hydroxyl radicals. Water Res 33, 2265–2276.
Wittmer, A., Heisele, A., McArdell, C.S., Böhler, M., Longree, P., Siegrist, H., 2015. Decreased UV absorbance as an indicator of micropollutant removal efficiency in wastewater treated with ozone. Water Sci. Technol. 71, 980–985.